

Modes of a Pure Ion Plasma at the Brillouin Limit

R. G. Greaves, M. D. Tinkle, and C. M. Surko

Physics Department, University of California, San Diego, La Jolla, California 92093

(Received 8 June 1994)

Ion plasma confinement and collective modes are investigated in a quadrupole Penning trap. The trap is operated in a novel steady-state mode, using an electron beam passing through the trap to ionize a low-pressure gas. We have discovered a regime of operation in which a Brillouin-density spheroidal ion plasma is produced. Azimuthally propagating modes are found to be in good agreement with a simple fluid model. This technique provides a new method for studying trapped plasmas near the density limit.

PACS numbers: 52.25.Wz, 52.35.Fp, 52.35.Nx

The confinement properties and collective modes of single-component plasmas are of fundamental interest and have been studied extensively, both theoretically and experimentally [1–9]. A basic feature of such plasmas is the existence of a maximum achievable density, first described by Brillouin [10], below which the repulsive and centrifugal forces on the rotating plasma can be balanced by the force due to the confining magnetic field. A unique feature of plasmas at the Brillouin limit is that the effective magnetic field vanishes, and the plasmas behave as though they are electrostatically confined. In the reference frame rotating with the plasma, particles execute straight-line orbits in the interior of the plasma and are reflected by the sheath at the plasma boundary [4,11]. Plasmas at the Brillouin limit have been studied in beams [12], but there have been relatively few reports relating to trapped plasmas.

The Brillouin density limit is a fundamental restriction on the maximum achievable density of a single-species plasma, and it is critical to many applications. For example, it represents the most stringent limitation on alternative fusion energy concepts based on Penning traps, and a significant theoretical and experimental effort has recently been directed at developing techniques for overcoming this restriction [13,14]. Dense trapped plasmas are now being developed as targets for high energy beam experiments [15]. Dense ion plasmas have also been proposed as a method of trapping and cooling positrons for the production of low-emittance beams [16]. Finally, the Brillouin limit places a practical restriction on the accumulation of antiprotons for antimatter studies [17].

Among the predicted modes of non-neutral plasmas are diocotron waves near multiples of the plasma rotation frequency, ω_r , and modes near the cyclotron frequency, $\Omega_c = qB/Mc$, where B is the magnetic field, c is the speed of light, and q and M are the charge and mass of the plasma particles, respectively. While low-frequency modes such as the diocotron mode and the Trivelpiece-Gould mode have been studied extensively in non-neutral plasmas [2–4], there have been few studies of the cyclotron modes [5,6], which have inconveniently high frequencies in typical electron plasmas.

Most experiments on single-component plasmas have been performed with pure electron plasmas, in which the Brillouin-density limit is difficult to achieve. The Brillouin limit has, however, been attained in a few experiments with ion plasmas. Dimonte reported observations of Trivelpiece-Gould modes in a lithium ion plasma [2], while Bollinger *et al.* studied the quadrupole upper hybrid mode in spheroidal ion plasmas in a Penning trap [9] and also indirectly observed an azimuthally asymmetric mode.

We have recently developed a new steady-state mode of operation of a quadrupole trap that enables us to explore a range of plasma phenomena including plasma confinement and both cyclotron and diocotron modes in pure ion plasmas near the Brillouin density. These experiments provide the first direct measurements of azimuthal modes in non-neutral plasmas near the Brillouin limit, and they complement the mode studies carried out in precision quadrupole traps [9]. Such plasma modes are also important to ion cyclotron resonance mass spectrometry, where an understanding of plasma effects could allow the larger signals available from dense plasmas to be used for precision ion mass measurements [18].

The understanding of plasma modes can also provide diagnostic information. For example, the diocotron mode frequency of a cylindrical plasma is often used to obtain the line charge density, and low-order modes are being developed as diagnostics of the temperature and aspect ratio of spheroidal plasmas [7–9,19]. Such diagnostics are expected to be important for monitoring the antimatter plasmas now under study [17,20].

The experiments were performed in a Penning trap designed to accumulate low-energy positrons [20]. A magnetic field of up to 1.3 kG is aligned with the electrode structure shown in Fig. 1, which approximates the hyperboloidal electrodes of a precision quadrupole trap. The ring electrode is split azimuthally into eight sectors set to a potential $-V$, while the two end-cap electrodes are set to V . The potential inside the trap is then $\Phi(\rho, z) \cong V(z^2 - \frac{1}{2}\rho^2)/z_0^2$, where $\rho = (x^2 + y^2)^{1/2}$ is the cylindrical radius, $z_0 = 6.3$ cm is the distance to the end caps from the center of the trap, and $\rho_0 = \sqrt{2}z_0$ is the inner radius of the ring electrode. A single trapped

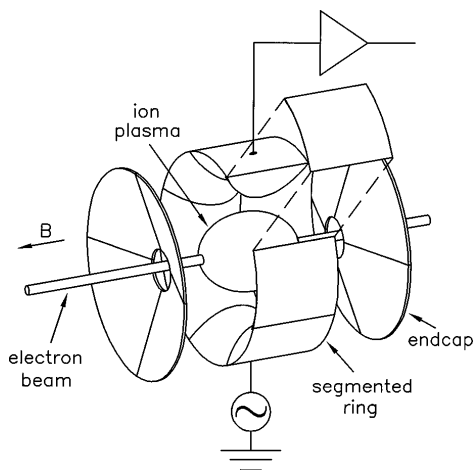


FIG. 1. Exploded view of the Penning trap used for these experiments, showing the segmentation of the ring electrode used to study azimuthal modes.

ion undergoes an axial oscillation at a frequency $\omega_z = (2qV/Mz_0^2)^{1/2}$ and an azimuthal rotation at the magnetron frequency, Ω_M , defined by $\omega_z^2 = 2\Omega_M(\Omega_c - \Omega_M)$.

Ions are continuously generated *in situ* by passing an electron beam along the trap axis in the presence of a gas at a pressure of $p \approx 10^{-7}$ torr. For a beam current of $i_B = 10 \mu\text{A}$ and a beam energy of about 100 eV, the ion production rate is of the order of 10^9 s^{-1} . Plasma losses are mainly due to collisions with the neutral gas, which set the confinement time to about 1 s.

The confinement of ions in the trap is subject to some interesting constraints. The quadrupole trap field prevents the confinement of even a single ion if V exceeds a critical value, $V_c = B^2 z_0^2 q / 4Mc^2$, at which $\omega_z^2 = \Omega_c^2 / 2$. Similarly, plasma self-fields limit the number density, n , of trapped ions to the Brillouin density, n_B , at which the plasma frequency, $\omega_p = (4\pi q^2 n / M)^{1/2}$, satisfies the condition $\omega_p^2 = \Omega_c^2 / 2$. For argon ions at a magnetic field of 1.3 kG, the density limit is $1.1 \times 10^6 \text{ cm}^{-3}$, which is quickly reached because of the high ion production rate and the relatively long confinement time.

The low-temperature thermal equilibrium of a small single-component plasma in a quadrupole trap is a uniform-density spheroid satisfying the relation [9]

$$\omega_p^2 = \omega_z^2(\alpha^2 - 1) / Q_1^0(k_2), \quad (1)$$

where $k_2 = \alpha / (\alpha^2 - 1)^{1/2}$ and $Q_1^0(k_2)$ is a Legendre function of the second kind. The plasma aspect ratio is $\alpha = L / 2r_p$, where L is the length of the plasma and r_p is its radius. The plasma rotates rigidly at a frequency, ω_r , which is related to the plasma frequency and the cyclotron frequency by the equation $\omega_p^2 = 2\omega_r(\Omega_c - \omega_r)$.

In analyzing our data, we have developed the following model to describe the plasma. After the electron beam is switched on and ions begin to accumulate, space charge causes the plasma to elongate. Except for very low values of V , not explored in this experiment, the density reaches the Brillouin limit before the plasma extends to the

end caps. Then, the plasma maintains a constant aspect ratio [determined by Eq. (1), and the condition $n = n_B$], expanding both radially and axially until it contacts one of the electrodes, which thereafter collects the excess ions. For a particular value of V , $V_t = (2 - \pi/2)V_c$, the aspect ratio is $\alpha = 1/\sqrt{2}$, and the plasma contacts both the ring electrode and the end caps. For $V < V_t$, the plasma length is fixed at $L = 2z_0$, and excess ions leave through the end caps. As a result of collisions, some ions will be transported radially out of the Brillouin-density core and will diffuse to the ring electrode, forming a tenuous halo plasma surrounding the core. For $V > V_t$, the plasma radius is fixed at $r_p = \rho_0$, and there is no halo plasma.

It would be desirable to measure the plasma profiles directly by dumping the plasma onto collector plates. However, this technique is not applicable here because most of the charge dumped is intercepted by the end caps, and furthermore, the orbits in a Brillouin-density plasma are large, so the particles do not stream out along field lines. We have developed two techniques that enable us to monitor the plasma shape indirectly by measuring currents to the electrodes.

The total charge in the trap can be obtained by measuring the image charge flowing onto the confining electrodes as the trap fills. Because the filling is rapid ($\tau \sim 100$ ms), a transient current is produced on the ring electrode when the electron beam is switched on. For $V < V_t$, this transient is clearly distinguishable from the dc current that is established once the trap has been filled. A typical current trace, obtained using an electrometer, is shown as an inset to Fig. 2. The total charge is obtained by integrating the current transients from all electrodes and correcting for the contribution from the image charge of the beam, which causes the small negative transient seen in the inset at $t = 0$. Figure 2 shows how the stored charge increases with V for an argon plasma with $B = 1.3$ kG. For $V > 10$ V, the transient wave form becomes more complicated, leading to some uncertainty in the analysis. The data points represent the charge obtained using a uniform method of analysis for all data, while the error bars represent an absolute lower bound. Using the model described above, the total charge in the Brillouin core is expected to be $Q = 4\pi r_p^3 \alpha n_B / 3$, which is shown by the solid line in Fig. 2.

In steady state, plasma equilibria can also be investigated indirectly by monitoring the dc current to the ring electrode. The inset to Fig. 3 shows how the ring current varies as the confining voltage is increased. For low values of V , the ring current is small. In our model, this condition corresponds to the case where the core plasma is not in contact with the ring, and most excess ions leave via the end caps. As V is increased, the plasma expands radially, and at some threshold voltage, an abrupt increase in the ring current is observed. Figure 3 shows the measured value of this threshold voltage as a function of magnetic field for four ion species. Also shown in this figure are the expected dependences, $V_t = (2 - \pi/2)V_c$, based

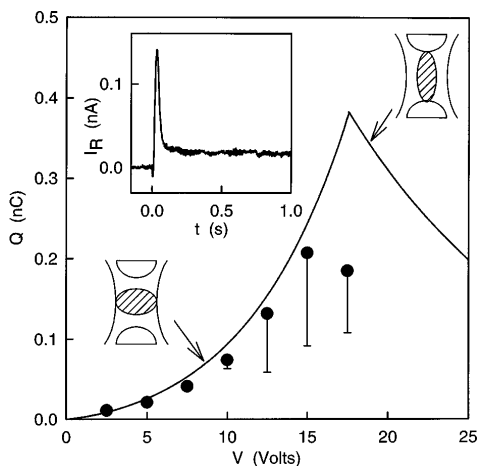


FIG. 2. Charge contained in the trap for an argon ion plasma, measured by integrating the current transient to the electrode when the electron beam is first switched on; $B = 1.3$ kG, $i_B = 10 \mu\text{A}$, $p \approx 1.0 \times 10^{-7}$ torr. Solid line: charge expected for a spheroidal ion plasma at the Brillouin limit. Inset: typical raw data showing the current to the ring electrode for $V = 5$ V.

on the model described above. No fitted parameters are used. The agreement between the model and the experiment, both for the total charge and for the ring current threshold, is consistent with the contention that most of the charge is contained in a plasma core at a density near n_B , with a diffuse halo plasma.

Plasma modes are excited by applying a signal to one of the ring sectors and detecting the plasma response on the opposite sector, as shown in Fig. 1. The beam energy is adjusted to reduce the production of doubly ionized particles, which are preferentially confined for $V > V_t$. Frequency spectra are measured using a spectrum analyzer

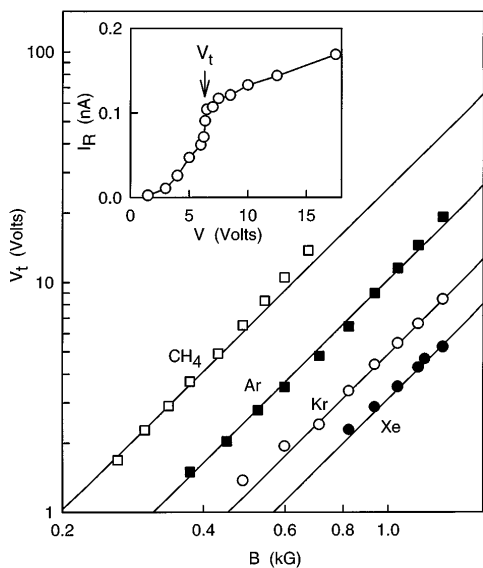


FIG. 3. Dependence of transition voltage on B for several ion species, with $i_B = 2.5 \mu\text{A}$. The solid lines show the behavior expected for a spheroidal ion plasma at the Brillouin limit. Inset: ion current to the ring electrode as a function of V for argon with $B = 0.82$ kG, showing the transition voltage, V_t .

and a tracking generator. Figure 4 shows the mode frequencies for an argon ion plasma as a function of V . It is clear that the character of the modes changes at $V = V_t$. For low values of V , two families of modes are discernible. One family has frequencies near Ω_c and has some similarity to the modes studied by Gould and LaPointe [5] in electron plasmas, while the low-frequency family consists of diocotron modes.

The plasma modes that should be most strongly excited by this technique are the purely azimuthal modes. The cold fluid dispersion relation for such modes in uniform-density cylindrical ion plasmas is [4]

$$2\omega_m = 2(m - 1)\omega_r + \Omega_c \pm [(\Omega_c - 2\omega_r)^2 + 2\omega_p^2 G_m]^{1/2} \quad (2)$$

for azimuthal mode number m , where $G_m = 1 - (r_p/r_w)^{2m}$ and r_w is the wall radius. In the notation of Ref. [1], these are the (m, m) modes. The plus and minus signs in Eq. (2) give solutions ω_m^+ and ω_m^- , corresponding to the cyclotron and diocotron branches of the dispersion relation, respectively. For the spheroidal case relevant to our experiment (but neglecting image charges) Dubin [1] was able to derive an analytic dispersion relation which has the same form as Eq. (2) but with the geometrical factor depending on α :

$$G_m = 2 \left[m - \frac{Q_m^m(k_2)}{\alpha(\alpha^2 - 1)^{1/2} Q_m^m(k_2)} \right]^{-1} \quad (3)$$

G_m varies from 0 to 1 as α varies from 0 to ∞ .

We cannot measure the rotation frequency ω_r directly. However, an experimental estimate of ω_r that is independent of the model chosen for G_m may be obtained from

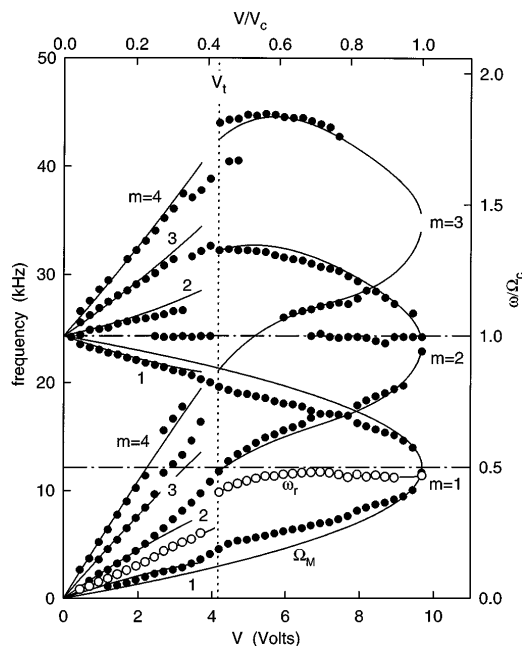


FIG. 4. Azimuthal mode frequencies vs V in an argon ion plasma, with $B = 640$ G. (\bullet): measured frequencies; (\circ): rotation frequency deduced from the data, as described in the text. The solid lines are from Eq. (2).

Eq. (2) by adding measurements of the frequencies of the cyclotron and diocotron modes for a particular mode number $m > 1$: $\omega_r = (\omega_m^+ + \omega_m^- - \Omega_c)/(2m - 2)$. The open circles in Fig. 4 represent the value of ω_r obtained by applying this procedure to the observed mode frequencies, using $m = 2, 3$, and 4 modes for $V < V_t$ and the $m = 2$ and 3 modes for $V > V_t$. Where more than one pair of modes was available, the estimates of ω_r were in good agreement. The m values were verified experimentally for the $m = 1, 2$, and 3 modes for $V < V_t$ and for the $m = 1$ and 2 modes for $V > V_t$.

Consider now the modes for $V < V_t$. As shown in Fig. 4, the inferred rotation frequency (shown by open circles) is close to $2\Omega_M$, rather than $\Omega_c/2$, which would characterize the Brillouin core. We interpret this to mean that the observed modes are supported in the halo plasma, which effectively shields the core. Using these inferred rotation frequencies, we find that the frequency data may be fitted by Eq. (2) by assuming $\omega_p^2 G_m = K_m \omega_z^2$, where $K_1 = 0.69$ and $K_m = 1.24$ for $m > 1$. The solid curves shown in Fig. 4 for $V < V_t$ are the results of this fit. The implications of this fit and of the observation that $\omega_r \approx 2\Omega_M$ for the nature of the halo plasma are not understood at present.

For $V > V_t$, the ring current data lead us to believe that the entire plasma can be described as a uniform-density spheroid with $n \approx n_B$. In fact, the estimated rotation frequency shown in Fig. 4 implies that n varies from $0.96n_B$ to greater than $0.99n_B$ for all values of V above V_t . We can calculate α explicitly from Eq. (1) and apply the result to Eq. (3) to obtain $G_m(\alpha)$. The mode frequencies can then be calculated using Eq. (2), and these results are shown in Fig. 4 by the solid lines for $V > V_t$. These calculations are in good agreement with the data, without using any fitted parameters, except for the $m = 1$ modes. This discrepancy could result from the effects of image charge, which are not included in the model and which are expected to be most pronounced for modes with the lowest m numbers. We note, however, that the sum of the frequencies of the $m = 1$ modes is close to Ω_c , which could account for the excitation of the weak mode observed near Ω_c , via a nonlinear coupling. We note also that a mode coupling occurs between the $m = 1$ cyclotron mode and the $m = 2$ diocotron mode near $V = 0.75V_c$.

In conclusion, we have demonstrated that plasmas near the Brillouin limit can be produced and studied for a variety of ion species, using an unusual steady-state mode of operation of a Penning trap. This technique produces spheroidal plasmas with density $n \approx n_B$, and aspect ratio varying with V . We have made the first direct measurements of azimuthally propagating modes in such a plasma. We have found that these modes can be described by a simple fluid model for V greater than some transition voltage, corresponding to a condition in which the Brillouin plasma extends radially to the

confining electrode. The dependence of n_B on B^2 means that for technologically feasible magnetic fields of about 100 kG, densities of $2.6 \times 10^{11} \text{ cm}^{-3}$ protons could be attained. Such densities are useful for many purposes, for example, as targets for beam experiments. More ambitious applications, such as fusion energy, would require the development of techniques for exceeding the Brillouin limit [13,14].

This new approach to the creation and study of pure ion plasmas is a promising extension of non-neutral plasma research. We expect that the technique could be implemented easily in other devices and configurations, such as the multipole traps that have been proposed for exceeding the Brillouin limit [14], opening up the possibility of new insights into the unusual physics of this regime.

We are pleased to acknowledge helpful conversations with D. H. E. Dubin, J. J. Bollinger, R. W. Gould, and the technical assistance of E. A. Jerzewski. This work is supported by the Office of Naval Research.

-
- [1] D. H. E. Dubin, Phys. Rev. Lett. **66**, 2076 (1991).
 - [2] G. Dimonte, Phys. Rev. Lett. **46**, 26 (1981).
 - [3] J. H. Malmberg and J. S. deGrassie, Phys. Rev. Lett. **35**, 577 (1975).
 - [4] R. C. Davidson, *Physics of Nonneutral Plasmas* (Addison-Wesley, Redwood City, CA, 1990).
 - [5] R. W. Gould and M. A. LaPointe, Phys. Rev. Lett. **67**, 3685 (1991).
 - [6] E. Sarid, F. Anderegg, and C. F. Driscoll, Bull. Am. Phys. Soc. **38**, 1971 (1993).
 - [7] C. S. Weimer *et al.*, Phys. Rev. A **49**, 3842 (1994).
 - [8] M. D. Tinkle *et al.*, Phys. Rev. Lett. **72**, 352 (1994).
 - [9] J. J. Bollinger *et al.*, Phys. Rev. A **48**, 525 (1993).
 - [10] L. Brillouin, Phys. Rev. **67**, 260 (1945).
 - [11] T. M. O'Neil, AIP Conf. Proc. **175**, 1 (1988).
 - [12] A. J. Theiss, R. A. Mahaffey, and A. W. Trivelpiece, Phys. Rev. Lett. **35**, 1436 (1975).
 - [13] L. Turner and D. C. Barnes, Phys. Rev. Lett. **70**, 798 (1993); K. Avinash and S. N. Bhattacharyya, Phys. Fluids B **4**, 3863 (1992); D. C. Barnes, R. A. Nebel, and L. Turner, Phys. Fluids B **5**, 3651 (1993); L. Turner *et al.*, Bull. Am. Phys. Soc. **38**, 1976 (1993).
 - [14] T. N. Tiourine, L. Turner, and A. W. C. Lau, Phys. Rev. Lett. **72**, 1204 (1994).
 - [15] R. E. Pollock (private communication).
 - [16] D. J. Wineland, C. S. Weimer, and J. J. Bollinger, Hyperfine Interact. **76**, 115 (1993).
 - [17] G. Gabrielse, S. L. Rolston, and L. Haarsma, Phys. Lett. A **129**, 38 (1988).
 - [18] J. B. Jeffries, S. E. Barlow, and G. H. Dunn, Int. J. Mass Spectrom. Ion Processes **54**, 169 (1983).
 - [19] J. J. Bollinger, D. J. Wineland, and D. H. E. Dubin, Phys. Plasmas **1**, 1403 (1994).
 - [20] R. G. Greaves, M. D. Tinkle, and C. M. Surko, Phys. Plasmas **1**, 1439 (1994).